

7N-39  
197138  
418

# TECHNICAL NOTE

## D-117

OPTIMUM DESIGN OF INSULATED TENSION MEMBERS

SUBJECTED TO AERODYNAMIC HEATING

By John R. Davidson

Langley Research Center  
Langley Field, Va.

NATIONAL AERONAUTICS AND SPACE ADMINISTRATION

WASHINGTON

December 1959

(NASA-TN-D-117) OPTIMUM DESIGN OF INSULATED  
TENSION MEMBERS SUBJECTED TO AERODYNAMIC  
HEATING (NASA) 41 p

N89-70635

Unclas  
00/39 0197138

W

NATIONAL AERONAUTICS AND SPACE ADMINISTRATION

---

TECHNICAL NOTE D-117

---

OPTIMUM DESIGN OF INSULATED TENSION MEMBERS

SUBJECTED TO AERODYNAMIC HEATING\*

By John R. Davidson

L  
5  
5  
1

SUMMARY

A general method for determining the weight efficiency of insulated heat-sink structures is developed by which the lightest total structural weight may be found for any selected insulating and load-carrying materials. In order to simplify the analysis, a constant temperature was assumed at the outside surface of the insulation. It is shown that an optimum structural weight exists for every combination of load, insulating material, structural material, and flight time. A load parameter has been found through which it is possible to compute efficiency curves for the load-carrying materials without specifying the insulation and flight time. Charts are presented for the optimum temperatures and optimum total structural weights for beryllium, HK31A magnesium, 2024-T4 aluminum, MST 185 titanium, 17-7PH stainless steel, and Inconel X based on an initial temperature of 75° F.

The results show that beryllium is an excellent insulated heat-sink structural material because of its light weight and high thermal capacity. If beryllium is excepted, titanium is most efficient for short flight times and high loads; as the flight time increases and the load decreases, stainless steel and Inconel X become the most efficient materials. The results also show that, in certain ranges, the uninsulated structure is more efficient. In general, insulated heat-sink structures are most efficient where the load is high and the flight time is short.

INTRODUCTION

The high temperatures encountered in high-speed flight can reduce the strength of unprotected structural materials. For very high temperatures the required increase in the size of unprotected members to maintain

---

\*The information presented herein was offered as part of a thesis in partial fulfillment of the requirements for the degree of Master of Science in Applied Mechanics, Virginia Polytechnic Institute, Blacksburg, Va., August 1958.

sufficient strength may be impractical, and it will become necessary to devise some means to insulate or cool the structure. The type of protection chosen will depend upon the aircraft, the thermal environment, and the load to be carried. No one type of design will be universally applicable, because some will be more efficient than others for specific flight conditions.

This paper will consider the insulated heat-sink type of structure where insulation between the airstream and the structure retards the flow of heat and delays the temperature rise of the metal. As a measure of efficiency, the criterion considered herein will be the total weight of the structure, which is the combined weight of the insulation and the metal.

By varying the thickness of the insulation layer, the temperature of the load-carrying structure can be maintained below any desired value. Because the weight of the insulation contributes to the overall design weight, it is inefficient from the weight standpoint to try to maintain excessively low temperatures by using large amounts of insulation. Thus, for any particular application, it is desirable to choose the thickness of the insulation and, consequently, the maximum temperature of the structure, in such a way that the combined weight of insulation and structure is a minimum.

The purpose of this study is to determine the basic parameters for evaluating the efficiency of insulated heat-sink structures and to determine the parameters that affect the design of the optimum structure for a simple aerodynamic-heating case.

#### SYMBOLS

|   |   |
|---|---|
| b | width, ft                                   |
| c | heat capacity, Btu/lb-°F                    |
| G | radiation geometry factor                   |
| h | heat-transfer coefficient, Btu/sq ft-sec-°F |
| k | thermal conductivity, Btu/ft-sec-°F         |
| P | total load, lb                              |
| q | thermal flux density, Btu/sq ft-sec         |
| T | temperature, °R or °F                       |

|            |  |
|------------|--|
| t          | thickness, ft  |
| W          | weight per square foot, lb/sq ft   |
| $\alpha_i$ | intercept of stress-temperature curve at $T = 0$   |
| $\beta_i$  | slope of stress-temperature curve when plotted semi-logarithmically                      |
| $\rho$     | weight density, lb/cu ft   |
| $\sigma$   | stress, lb/sq ft; or Stefan-Boltzmann constant   |
| $\sigma_y$ | yield stress at 0.2-percent offset, lb/sq ft   |
| $\tau$     | time, sec  |
| $\Omega$   | load parameter, $\left(\frac{P}{b}\right)^2 \frac{1}{k_1 \rho_1 \tau}$ , sq ft-lb-°F/Btu |
| exp        | exponent to base $e = 2.718$   |

#### Subscripts:

|     |  |
|-----|--|
| a   | surroundings   |
| aw  | adiabatic wall   |
| eq  | equilibrium  |
| 0   | initial conditions   |
| 1   | refers to insulation properties or initial (left) section of stress-temperature curve        |
| 2   | refers to primary structure properties or second (right) section of stress-temperature curve |
| i   | indicial notation  |
| opt | maximum metal temperature $T_2$ of an optimum structure                                      |
| r   | radiated   |
| c   | conducted  |

Primed symbols indicate iterated values.

## PROCEDURE

Figure 1 shows the configuration which will be analyzed. Several assumptions are made to simplify the analysis:

- (1) The heating is uniform over the entire surface of the member; that is, the heat flow is one dimensional
- (2) The metal structure carries the entire load
- (3) The temperature gradient through the metal structure is so small that it can be neglected
- (4) The thermal capacity of the insulation layer is so much smaller than the thermal capacity of the structure that its effect can be neglected. (Appendix A gives a method for improving this approximation for larger thicknesses of insulation.)
- (5) At the start of flight the outside surface of the insulation is suddenly raised from the initial temperature of  $T_0$  to a constant temperature  $T_{eq}$
- (6) The heat capacity and thermal conductivity are constant.

The thermal environment will determine the temperature at the outside of the insulation. This temperature will closely approach the recovery temperature of the airstream (sometimes called the adiabatic wall temperature) when losses due to radiation are neglected. When radiation is considered, this temperature will be somewhat lower. In appendix B an approximate method for determining this temperature is given. Reference 1 contains an exact solution to the insulated-slab temperature distribution problem and discusses the effects of some of these assumptions on the temperature rise of the load-carrying structure.

The weight per square foot of the protected structure including the insulation is

$$W = \rho_1 t_1 + \rho_2 t_2 \quad (1)$$

All members considered for a given application have the same length and width and are required to carry the same tensile load under the same environmental conditions. Of the many possible choices of  $t_1$  and  $t_2$  and available structural material, a combination which results in the lightest structure is to be found.

The load which is supported by the member is

$$P = \sigma b t_2$$

The largest load which can be carried for a given thickness is

$$P = \sigma_y b t_2 \quad (2)$$

where the yield stress at 0.2 percent (strainwise) offset at 1/2 hour exposure to temperature has been assumed as the maximum allowable stress. The thickness required to support this load is

$$t_2 = \frac{P}{\sigma_y b} \quad (3)$$

It should be noted that  $\sigma_y$  is a function of the material, temperature, time of exposure to temperature, and strain rate. Since short times of exposure are considered herein, the exposure time was taken as 1/2 hour where data were available at conventional strain rates between 0.002 and 0.005 inch per inch per minute. (See refs. 2 to 7.) With these considerations, the yield stress is primarily dependent upon temperature, as shown in figure 2. The solid lines through the experimental points show that this dependence may be expressed empirically by the sectional representation

$$\log_e \sigma_y = \log_e \alpha_i - \beta_i T \quad (i = 1, 2) \quad (4a)$$

or, in an alternate form

$$\sigma_y = \alpha_i e^{-\beta_i T} \quad (4b)$$

where  $\alpha_i$  is the intercept at the ordinate when  $T = 0$ , and  $\beta_i$  is the slope of the curve for  $\sigma_y$  plotted against  $T$ . The indicial notation is used to denote the respective sections of the curve; the subscript 1 refers to the lower temperature portion, and the subscript 2 refers to the higher temperature portion.

Substitution of equation (4b) into equation (3) gives the load-carrying structure thickness as a function of temperature

$$t_2 = \frac{P}{b \alpha_i e^{-\beta_i T_2}} \quad (5)$$

where  $T_2$  is the temperature of the load-carrying material.

The temperature of the structure is dependent upon the thickness of the insulation, the thickness of the structure, and the temperature at the outside surface of the insulation. Since the thermal capacity of the insulation is neglected, all the heat entering the outside surface of the insulation must go through to the structure. The heat entering is proportional to the difference in the temperature of the outside insulation surface and the primary structure. This relationship is expressed by the following differential equation:

$$\frac{k_1}{t_1}(T_{eq} - T_2) = c_2 \rho_2 t_2 \frac{dT_2}{d\tau} \quad (6)$$

If  $T_{eq}$  is considered independent of time, the solution of this equation is

$$\frac{T_{eq} - T_2}{T_{eq} - T_0} = \exp\left(\frac{-k_1 \tau}{c_2 \rho_2 t_2 t_1}\right) \quad (7)$$

which may be solved for the thickness to yield

$$t_1 = \frac{k_1 \tau}{c_2 \rho_2 t_2 \log_e \frac{T_{eq} - T_0}{T_{eq} - T_2}} \quad (8)$$

By using equations (5) and (8) the material thicknesses may be eliminated from equation (1).

$$W = \frac{\rho_2 P}{b \alpha_i e^{-\beta_i T_2}} + \frac{\rho_1}{\rho_2} \frac{k_1 \tau b \alpha_i e^{-\beta_i T_2}}{P c_2 \log_e \frac{T_{eq} - T_0}{T_{eq} - T_2}} \quad (9)$$

The weight is expressed in terms of the metal temperature because, once this temperature is known, the yield stress, and thus  $t_2$ , are fixed (by eq. (3)). The insulation thickness can then be determined from equation (8). The value of  $T_2$  that makes  $W$  a minimum may be determined by setting the partial derivative of  $W$  with respect to  $T_2$  equal to zero. The result, after some algebraic manipulation and the use of equation (7), is

$$\left(\frac{\sigma_y}{\rho_2}\right)^2 \left( \frac{1}{c_2 \log_e \frac{T_{eq} - T_0}{T_{eq} - T_2}} \right) \left[ 1 + \frac{1}{\beta_1 (T_{eq} - T_2) \log_e \frac{T_{eq} - T_0}{T_{eq} - T_2}} \right] = \left(\frac{P}{b}\right)^2 \frac{1}{k_1 \rho_1 \tau} = \Omega \quad (10)$$

The left-hand side of equation (10) contains the equilibrium temperature  $T_{eq}$ , optimum temperature  $T_2$ , and structural material properties.

On the other side is the load, flight time, and insulation properties. This convenient separation of insulation and metal properties permits the computation of the load parameter  $\Omega$  as a function of the equilibrium and initial temperatures, for any metal, regardless of the insulation which may be chosen. Figure 3 shows the results of such a computation for beryllium, magnesium, aluminum, titanium, stainless steel, and Inconel X. The weight densities and thermal capacities of the metals used for these computations are given in table I. The dashed line, which will be discussed later, shows the values of  $\Omega$  for various equilibrium temperatures below which it is more efficient not to insulate. In order to use the charts, the optimum temperature is found by first computing

$$\Omega = \left(\frac{P}{b}\right)^2 \frac{1}{k_1 \rho_1 \tau} \quad \text{for a specified load, insulation, and flight time, and}$$

then entering the chart for the primary structure material with this value and  $T_{eq}$  to find the optimum value of  $T_2$ . It should be noted that the discontinuity in the slope of the empirical sectional representation of the curve of  $\log_e \sigma_y$  plotted against temperature leads to a discontinuity in the optimum temperature curves. If test data are used, there is actually no discontinuity. A few computations using the test points were made to determine the shape of the optimum temperature curve in this vicinity; the remainder of the curves were faired in by making use of the properties of carpet plots.

Once the optimum temperature has been found, the metal thickness, insulation thickness, and total weight per square foot may be found from equation (3) and figure 2, equation (8b), and equation (1), respectively. For computational convenience these equations can be combined to give

$$\frac{Wb}{P} = \frac{\rho_2}{\sigma_y} \left[ 1 + \left(\frac{\sigma_y}{\rho_2}\right)^2 \frac{1}{\Omega c_2 \log_e \frac{T_{eq} - T_0}{T_{eq} - T_2}} \right] \quad (11)$$

where  $T_2$  is the optimum temperature found from figure (3) and  $Wb/P$  is the ratio of the total weight per square foot to the load per unit width. Values of  $Wb/P$  for beryllium, magnesium, aluminum, titanium,



stainless steel, and Inconel X are plotted in figure 4 against equilibrium temperature and loading parameter. Again, the dashed line represents the uninsulated structure. This line can be computed from equation (1) with  $t_1 = 0$  or from equation (11) with  $T_2 = T_{eq}$ ; the resulting equation is

$$\frac{Wb}{P} = \frac{\rho_2}{\sigma_y} \quad (12)$$

Figure 4 shows that the total weight per unit load increases as  $\Omega$  decreases, until, when the load becomes small enough (a small load means small thermal capacity), it becomes more efficient not to insulate and to use a relatively thick primary structure at the equilibrium temperature instead of a cooler, thinner, primary structure covered with a very thick blanket of insulation.

For purposes of comparison, the relative efficiencies of the uninsulated materials are shown in figure 5. This figure indicates that, for uninsulated structures of the materials considered herein with equilibrium temperatures less than  $400^\circ \text{F}$ , MST 185 titanium is the most efficient; for  $400^\circ \text{F} < T_{eq} < 1,130^\circ \text{F}$ , beryllium becomes most efficient; and above  $1,130^\circ \text{F}$ , Inconel X is most efficient.

Figure 6 was drawn to illustrate the dependence of optimum temperature upon the load for a given choice of insulation, metal, flight time, and equilibrium temperature. Figure 6 was sketched from equation (9). This figure shows that there can be two points of zero slope, one a minimum weight and one a maximum weight. As the load decreases, the optimum temperature increases until, as is shown by the curve for  $(P/b)_3$ , there is a sudden jump to an end-point minimum where the lightest structure is designed to withstand the equilibrium temperature. For all loads less than  $(P/b)_3$  (for a given insulation, metal, flight time, and equilibrium temperature), the uninsulated structure will be more efficient. The point of zero slope that is a maximum moves closer to  $T_{eq}$  as the load increases and usually is within  $5^\circ \text{F}$  of  $T_{eq}$ . The point of minimum slope moves toward  $T_0$  as  $P/b$  increases; the minimum can occur anywhere between  $T_0$  and a few degrees below  $T_{eq}$ .

A comparison of the weight charts of figure 4 shows that beryllium would be the most efficient insulated structural material except for a small region where  $T_{eq} < 1,675^\circ \text{F}$  and  $\Omega < 4 \times 10^9$  where uninsulated Inconel X would be better. However, at present beryllium is not in wide use. If beryllium is excluded, the relative efficiencies of the remaining

materials are shown in figure 7. The figure was constructed by superposing the weight charts for the individual materials and noting where the lines of like  $T_{eq}$  crossed. This graphical technique, which used faired curves through computed points, led to an erratic boundary between titanium and stainless steel where (because there was little difference in the efficiency of these two materials in this region) the lines of constant adiabatic wall temperature were nearly parallel. Therefore, since the location of this boundary is not critical, a line of  $\Omega = \text{Constant}$  was chosen as the boundary.

If equations (3) and (8) are substituted into equation (10), the following equation results

$$\frac{W_2}{W_1} = \frac{\rho_2 t_2}{\rho_1 t_1} = 1 + \frac{1}{\beta_i (T_{eq} - T_2) \log_e \frac{T_{eq} - T_0}{T_{eq} - T_2}}$$

where  $W_1$  and  $W_2$  are the weights of the insulation layer and metal layer, respectively. It can be seen from this equation that the metal layer always weighs more than the insulation layer in an optimum structure for the constant-equilibrium-temperature case.

## PRESENTATION OF RESULTS

Two example problems will be used to illustrate the method of design and to show typical results.

### Example Problem I

The design conditions are:

$$P/b = 3 \times 10^4 \text{ lb/ft}$$

$$\tau = 60 \text{ sec}$$

$$T_{eq} = 1,200^\circ \text{ F}$$

$$T_0 = 75^\circ \text{ F}$$

For this first problem, an efficient insulation, such as a low density asbestos will be considered. (However, it should be noted that such a

material by itself has low strength and may need protection from the scrubbing action of a high-velocity airstream.) For the insulation,

$$k_1 = 2 \times 10^{-6} \text{ Btu/ft-sec-}^{\circ}\text{F}$$

$$\rho_1 = 20 \text{ lb/cu ft}$$

$$c_1 \approx 0.24 \text{ Btu/lb-}^{\circ}\text{F}$$

The load parameter  $\Omega$  is computed from equation (10) to be

$$\Omega = \left(\frac{P}{b}\right)^2 \frac{1}{k_1 \rho_1 \tau} = \frac{(3 \times 10^4)^2}{(2 \times 10^{-6})(20)(60)} = 3.75 \times 10^{11}$$

Figure 7 is entered with  $T_{eq} = 1,200^{\circ} \text{ F}$  and this value of  $\Omega$ . It is found that insulated titanium is the most efficient structural material, and that

$$\frac{Wb}{P} = 2.02 \times 10^{-5}$$

or

$$W = 2.02 \times 10^{-5} \left(\frac{P}{b}\right) = 2.02 \times 10^{-5} \times 3 \times 10^4 = 0.606 \text{ lb/sq ft}$$

From figure 4(d), the optimum temperature is

$$(T_2)_{opt} = 420^{\circ} \text{ F}$$

From equation (3) and figure 2

$$t_2 = \frac{P}{b\sigma_y} = \frac{3 \times 10^4}{1.77 \times 10^7} = 1.695 \times 10^{-3} \text{ ft} = 0.0203 \text{ in.}$$

The thickness of the insulation is found from equation (8)

$$\begin{aligned} t_1 &= \frac{k_1 \tau}{c_2 \rho_2 t_2 \log_e \frac{T_{eq} - T_0}{T_{eq} - T_2}} = \frac{(2 \times 10^{-6})(60)}{(0.118)(295)(1.695 \times 10^{-3}) \log_e \left( \frac{1200 - 75}{1200 - 420} \right)} \\ &= 5.66 \times 10^{-3} \text{ ft} = 0.0680 \text{ in.} \end{aligned}$$

Improved accuracy may be obtained through an iteration procedure which takes into account the insulating effect of the thermal capacity of the insulation. (See appendix A.) First compute

$$\frac{c_1 \rho_1 t_1}{c_2 \rho_2 t_2} = \frac{(0.24)(20)(5.66 \times 10^{-3})}{(0.118)(295)(1.695 \times 10^{-3})} = 0.4605$$

By definition (from eq. (A3))

$$k_1' = k_1 \left[ \frac{1}{1 + \frac{1}{2} \left( \frac{c_1 \rho_1 t_1}{c_2 \rho_2 t_2} \right)} \right] = (2 \times 10^{-6}) \left( \frac{1}{1.23} \right) = 1.625 \times 10^{-6}$$

The thermal capacity of the insulation has an effect similar to reducing the insulation conductivity by about 23 percent.

Repeating the computations and using primed symbols to indicate iterated values yields

$$\Omega' = \left( \frac{P}{b} \right)^2 \frac{1}{k_1' \rho_1 \tau} = \frac{(3 \times 10^4)^2}{(1.625 \times 10^{-6})(20)(60)} = 4.615 \times 10^{11}$$

$$\frac{W'b}{P} = 1.94 \times 10^{-5}$$

$$W' = (3 \times 10^4)(1.94 \times 10^{-5}) = 0.582 \text{ lb/sq ft}$$

$$(T_2')_{\text{opt}} = 390^\circ \text{ F}$$

$$t_2' = \frac{3 \times 10^4}{1.82 \times 10^7} = 1.648 \times 10^{-3} \text{ ft} = 0.0198 \text{ in.}$$

$$\begin{aligned} t_1' &= \frac{(1.625 \times 10^{-6})(60)}{(0.118)(295)(1.648 \times 10^{-3}) \log_e \frac{1200 - 75}{1200 - 390}} \\ &= 5.175 \times 10^{-3} \text{ ft} = 0.0621 \text{ in.} \end{aligned}$$

A second iteration yields

$$k_1'' = k_1 \frac{1}{1 + \frac{1}{2} \frac{c_1 \rho_1 t_1}{c_2 \rho_2 t_2}} = 1.644 \times 10^{-6}$$

From this value

$$\frac{W''b}{P} = 1.96 \times 10^{-5}$$

$$W'' = 0.588 \text{ lb/sq ft}$$

The iteration procedure results in a design that is about 4 percent lighter than the design where the thermal capacity of the insulation was neglected. Frequently, the thermal conductivity of the insulation is not known within 20 percent. Inaccuracies may be introduced through other thermal constants or through boundary values such as  $T_{eq}$ . These practical considerations show that in many cases the improved accuracy gained by iteration is unnecessary.

#### Example Problem II

The loading and flight conditions will remain the same as in problem I. However, for problem II an insulation with characteristics similar to a fiber glass laminate will be chosen. Typical values for such an insulation are

$$k_1 = 6 \times 10^{-5} \text{ Btu/ft-sec-}^{\circ}\text{F}$$

$$\rho_1 = 110 \text{ lb/cu ft}$$

$$c_1 = 0.24 \text{ Btu/lb-}^{\circ}\text{F}$$

From equation (10)

$$\Omega = \left(\frac{P}{b}\right)^2 \frac{1}{k_1 \rho_1 \tau} = \frac{(3 \times 10^4)^2}{(6 \times 10^{-5})(110)(60)} = 2.272 \times 10^9$$

From figure 7 it is found that uninsulated Inconel X is the most efficient material and that

$$\frac{Wb}{P} = 4.36 \times 10^{-5}$$

at the intersection of the  $T_{eq} = 1,200^\circ \text{ F}$  curve and the dashed line denoting uninsulated Inconel X.

$$W = (3 \times 10^4)(4.36 \times 10^{-5}) = 1.308 \text{ lb/sq ft}$$

and, at  $(T_2)_{opt} = 1,200^\circ \text{ F}$ ,

$$t_2 = \frac{P}{b} \frac{1}{\sigma_y} = \frac{3 \times 10^4}{1.7 \times 10^7} = 1.764 \times 10^{-3} \text{ ft} = 0.0212 \text{ in.}$$

#### DISCUSSION

The result of problem I indicates the use of MST 185 titanium alloy with low-density asbestos insulation is the best solution; the result of problem II indicates the use of uninsulated Inconel X with a resulting structure of twice the weight of that of problem I to be the best solution. Both problems were based on the same load and flight conditions. The apparent disparity of results is caused by considering insulations with such widely varying values of  $k_1 \rho_1$ . If an efficient insulation is available and if it will withstand the aerodynamic forces and temperatures, it will pay to use it. However, if the only suitable insulation has a high value of  $k_1 \rho_1$ , it will not be efficient to use it unless the equilibrium temperatures are very high or unless the loads are high and the flight times short. Figure 7 illustrates that efficient insulated structures are those with high values of  $\Omega$ , which reflect efficient insulations, short heating periods, and large thermal capacity available in the metal thickness.

The computed curves for weight and optimum temperature are based on an initial temperature of  $75^\circ \text{ F}$ . Curves can be computed for other values of initial temperature.

The method should be applicable to cases where the temperature of the insulation outside surface is monotonically increasing by using some other equation to express the thickness of the structure in terms of the temperature. However, it may not be possible in all cases to separate

the insulation properties from the structural material properties, as was done herein through the load parameter  $\Omega$ . In instances where the front surface temperature decreases after a period of rise, some care must be exercised. If the flight time is sufficiently long, there may be a period of cooling and the maximum structure temperature (upon which the allowable stress is based) might occur before the end of the flight.

#### CONCLUDING REMARKS

The results show that there is an optimum combination of insulation and load-carrying material thickness for which the combined weight of the insulating and structural materials is a minimum for a specified load, insulation, flight time, and constant temperature at the outside surface of the insulation. For a constant temperature at the insulation surface, it is possible to obtain a set of weight curves for optimum configurations for any specified structural material through the use of a load parameter which includes the load, insulation density and conductivity, and flight period.

For long flight times and low equilibrium temperatures (below 1,400° F) uninsulated structures may be more efficient than insulated structures. Insulated heat-sink structures are efficient when efficient insulating materials can be used, and when the load is large and the flight time is short.

Langley Research Center,  
National Aeronautics and Space Administration,  
Langley Field, Va., July 28, 1959.

## APPENDIX A

## SECOND APPROXIMATION TO THE TEMPERATURE EQUATION

An exact analysis of a heavily insulated thick plate is given in reference 1. This reference discusses two approximations to the exact solution. The first approximation, which neglects the thermal capacity of the insulation, was used in reference 1 and in this paper to express the structure thickness in terms of temperature. The derivation of the second approximation, which admits an effect due to the insulation thermal capacity, is given here.

The assumptions are as follows:

(1) The temperature at the outside surface of the insulation is raised immediately from  $T_0$  to  $T_{eq}$  at  $\tau = 0$ .

(2) There is no temperature gradient through the thickness of the structural material

(3) There is a linear temperature gradient through the thickness of the insulation.

The first two assumptions are the same as were made in the body of this paper for the first approximation. The third assumption is exactly true only in the steady-state case where the metal temperature is constant and after a time which is so long that initial transients have died out. It can be shown that the initial transients die out within a very short period. Therefore, this approximation is good if the metal temperature rises slowly.

The effective temperature of the insulation for the purposes of expressing stored heat is  $\frac{1}{2}(T_{eq} + T_2)$  as a result of assumption (3).

This expression leads to the following differential heat balance equation:

$$q = \frac{k_1}{t_1}(T_{eq} - T_2) = \left(\frac{1}{2} c_1 \rho_1 t_1 + c_2 \rho_2 t_2\right) \frac{dT_2}{d\tau} \quad (A1)$$



The solution to equation (A1) is

$$\frac{T_{eq} - T_2}{T_{eq} - T_0} = \exp \left[ \frac{-k_1 \tau}{c_2 \rho_2 t_2 t_1 \left( 1 + \frac{1}{2} \frac{c_1 \rho_1 t_1}{c_2 \rho_2 t_2} \right)} \right] \quad (A2)$$

Equation (A2) differs from equation (7) by an additional term of

$$\frac{1}{1 + \frac{1}{2} \frac{c_1 \rho_1 t_1}{c_2 \rho_2 t_2}}$$

in the right-hand exponential expression. Although equation (A2) is a better approximation to the exact solution than equation (7), it cannot be solved explicitly for the insulation thickness  $t_1$ , thus, the difficulty of mathematical manipulation is increased.

An iteration procedure will circumvent this difficulty and improve the accuracy of the analysis based on the first approximation. The additional thermal capacity retards the temperature rise of the metal in a manner similar to a decrease in the insulation thermal conductivity. Determine approximately the thicknesses  $t_1$  and  $t_2$  according to the analysis using the first approximation for the temperature  $T_2$  and then define

$$k_1' = k_1 \left( \frac{1}{1 + \frac{1}{2} \frac{c_1 \rho_1 t_1}{c_2 \rho_2 t_2}} \right) \quad (A3)$$

The new thermal conductivity  $k_1'$  is used to compute a new value of  $\Omega$ ; this value, in turn, is used to determine new values for  $t_1$  and  $t_2$ . The procedure is repeated until the difference between succeeding values of optimum weight are negligible. Usually about three iterations are sufficient.

A comparison of the second approximation with the exact solution to the temperature problem as presented in reference 1 shows that, if  $\frac{c_1 \rho_1 t_1}{c_2 \rho_2 t_2} \approx 1$ , the error at the beginning of the heating period is about  $1/10(T_{eq} - T_0)$  which is caused by the lag in temperature rise at the insulation outside surface. The approximate solution gives a higher

temperature rise than the exact solution. As the heating period progresses, the approximate solution reaches the exact solution at a time when  $T_2 = T_{eq} - 0.37(T_{eq} - T_0)$ . When  $T_2 = T_{eq} - 0.1(T_{eq} - T_0)$ , the approximate solution is  $0.015(T_{eq} - T_0)$  lower than the exact solution.

When  $\frac{c_1 \rho_1 t_1}{c_2 \rho_2 t_2} \approx \frac{1}{10}$ , the second approximation and the exact solution agree within  $0.005(T_{eq} - T_0)$  for times where  $T_2 \leq T_{eq} - 0.05(T_{eq} - T_0)$ .

The approximation improves as  $\frac{c_1 \rho_1 t_1}{c_2 \rho_2 t_2}$  approaches 0.

These comparisons with the exact solution were done for an aerodynamic-heating case without radiation where the aerodynamic heat-transfer coefficient contributed no significant retardation to the flow of heat, that is, where  $\frac{k_1}{ht_1} \ll 1$  where  $h$  is the aerodynamic heat-transfer coefficient.

## APPENDIX B

## DETERMINATION OF THE EQUILIBRIUM TEMPERATURE

The boundary layer of air at the insulation surface retards the conduction of heat into the surface. If, at the same time, the surface radiates heat to its surroundings, the insulating effect of the boundary layer may make possible surface temperatures greatly below the recovery temperature of the airstream. The heat-balance equation at the surface is

$$q = q_r + q_c \quad (B1)$$

where  $q$  is the heat flux conducted through the boundary layer,  $q_r$  is the heat radiated to the surroundings, and  $q_c$  is the heat conducted into the insulation and to the structure. This equation may be written as

$$\begin{aligned} h(T_{aw} - T_1) &= \sigma G(T_1^4 - T_a^4) + q_c \\ &\approx \sigma G(T_1^4 - T_a^4) + \frac{k_1}{t_1}(T_1 - T_2) \end{aligned} \quad (B2)$$

where  $\sigma$  is the Stefan-Boltzmann constant,  $G$  incorporates the radiation geometry and emissivities,  $h$  is the conductivity of the boundary layer,  $T_{aw}$  is the effective recovery temperature of the airstream, and  $T_1$  is the temperature of the outside surface of the insulation. (All temperatures are absolute.) For an aircraft radiating to space,  $T_a^4 \ll T_1^4$  and may be neglected. The heat flux into an insulated plate is small, and for values of  $T_1 \geq 2,000^\circ \text{R}$ ,  $q_c \ll \sigma G T_1^4$  and may be neglected.

Then

$$h(T_{aw} - T_1) = \sigma G T_1^4$$

or

$$T_{aw} = T_1 \left( 1 + \frac{\sigma G}{h} T_1^3 \right) \quad (B3)$$

The temperature  $T_1$  is at the outside surface of the insulation, and therefore

$$T_1 = T_{eq}$$

and equation (B3) becomes

$$T_{aw} = T_{eq} \left( 1 + \frac{\sigma G}{h} T_{eq}^3 \right) \quad (B4)$$

after a short initial transient period caused by the thermal capacity of the insulation.

L  
5  
5  
1

## REFERENCES

1. Davidson, John R.: Optimum Design of Insulated Tension Plates in Aerodynamically Heated Structures. M.S. Thesis. Virginia Polytechnic Inst., 1958.
2. Anon.: Report of the Panel on Beryllium of the Materials Advisory Board. Report MAB-129-M, June 25, 1958.
3. Anon.: HK31A Magnesium Alloy Sheet and Plate. Bull. No. 141-174, Magnesium Dept., The Dow Chemical Co.
4. Anon.: Strength of Metal Aircraft Elements. ANC-5 Bull., Rev. ed., Depts. of Air Force, Navy, and Commerce, Mar. 1955.
5. Anon.: MST Alloy Data Sheet - MST 1.3Al-8V-5Fe Titanium Alloy. Mallory-Sharon Titanium Corp., Apr. 25, 1957.
6. Kurg, Ivo M.: Tensile Stress-Strain Properties of 17-7 PH and AM 350 Stainless-Steel Sheet at Elevated Temperatures. NACA TN 4075, 1957.
7. Anon.: Inconel "X" - A High Strength, High Temperature Alloy, Data and Information. The International Nickel Co., Inc., Dev. and Res. Div., Jan. 1949.

TABLE I

## WEIGHT DENSITY AND HEAT CAPACITY FOR STRUCTURAL MATERIALS

[All values were considered as constants during computation of curves]

| Material                | Weight density, $\rho$ ,<br>lb/cu ft | Heat capacity, $c$ ,<br>Btu/lb-°F |
|-------------------------|--------------------------------------|-----------------------------------|
| Beryllium               | 115.8                                | 0.53                              |
| HK31A magnesium         | 112                                  | .247                              |
| 2024-T4 aluminum        | 175                                  | .23                               |
| MST 185 titanium        | 295                                  | .118                              |
| 17-7 PH stainless steel | 484                                  | .13                               |
| Inconel X               | 519                                  | .12                               |

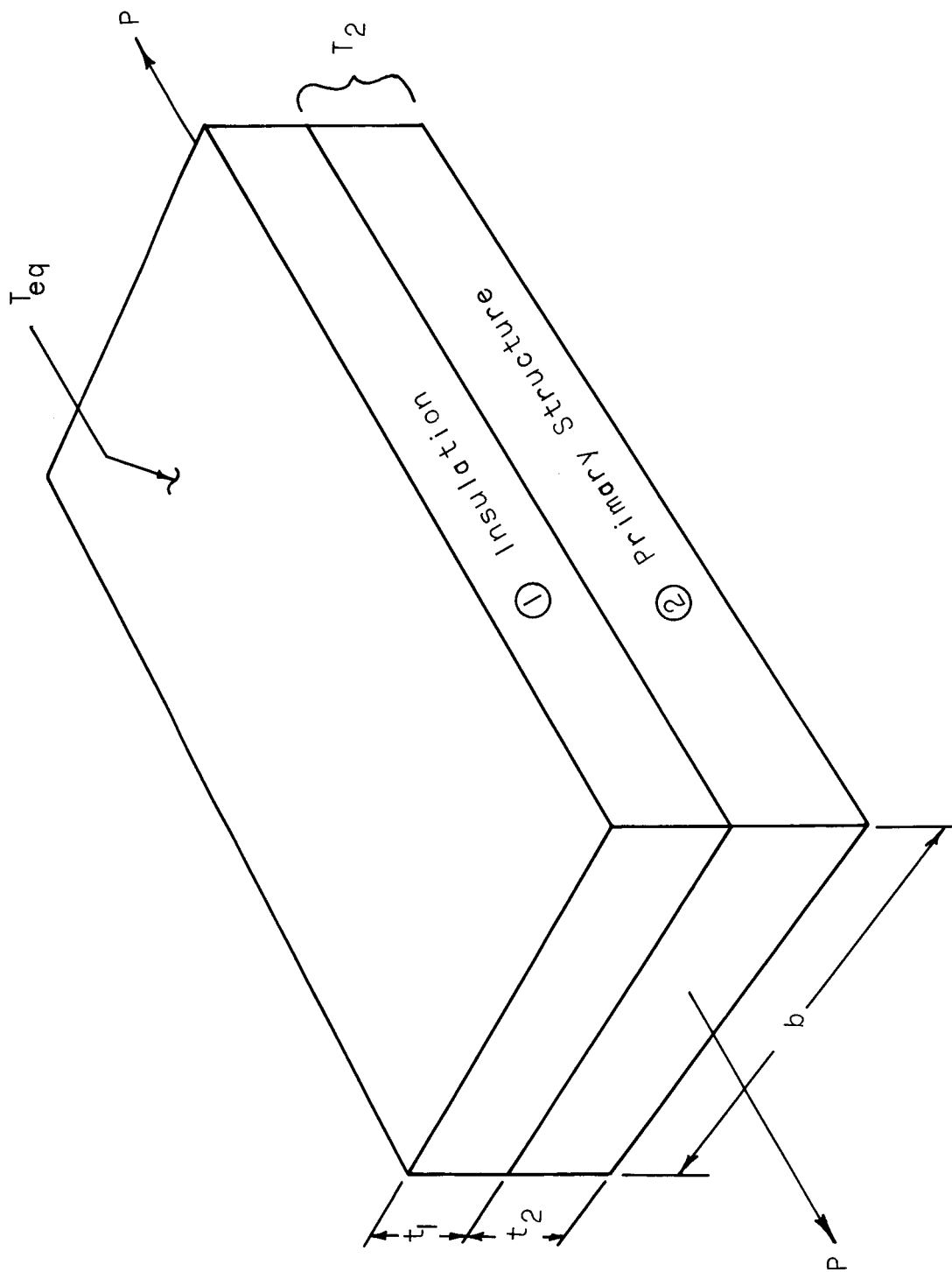


Figure 1.- Sketch of insulated structure.

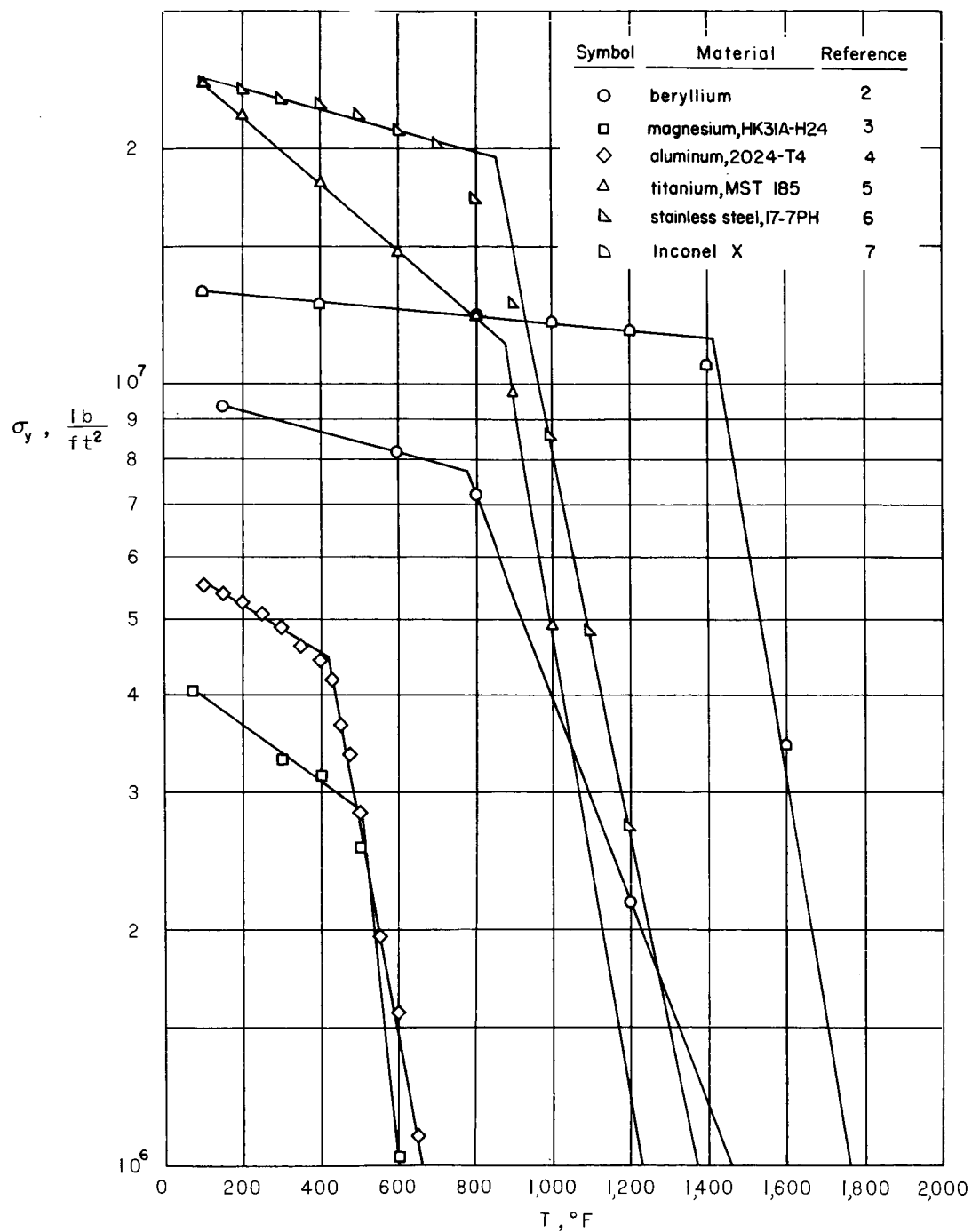
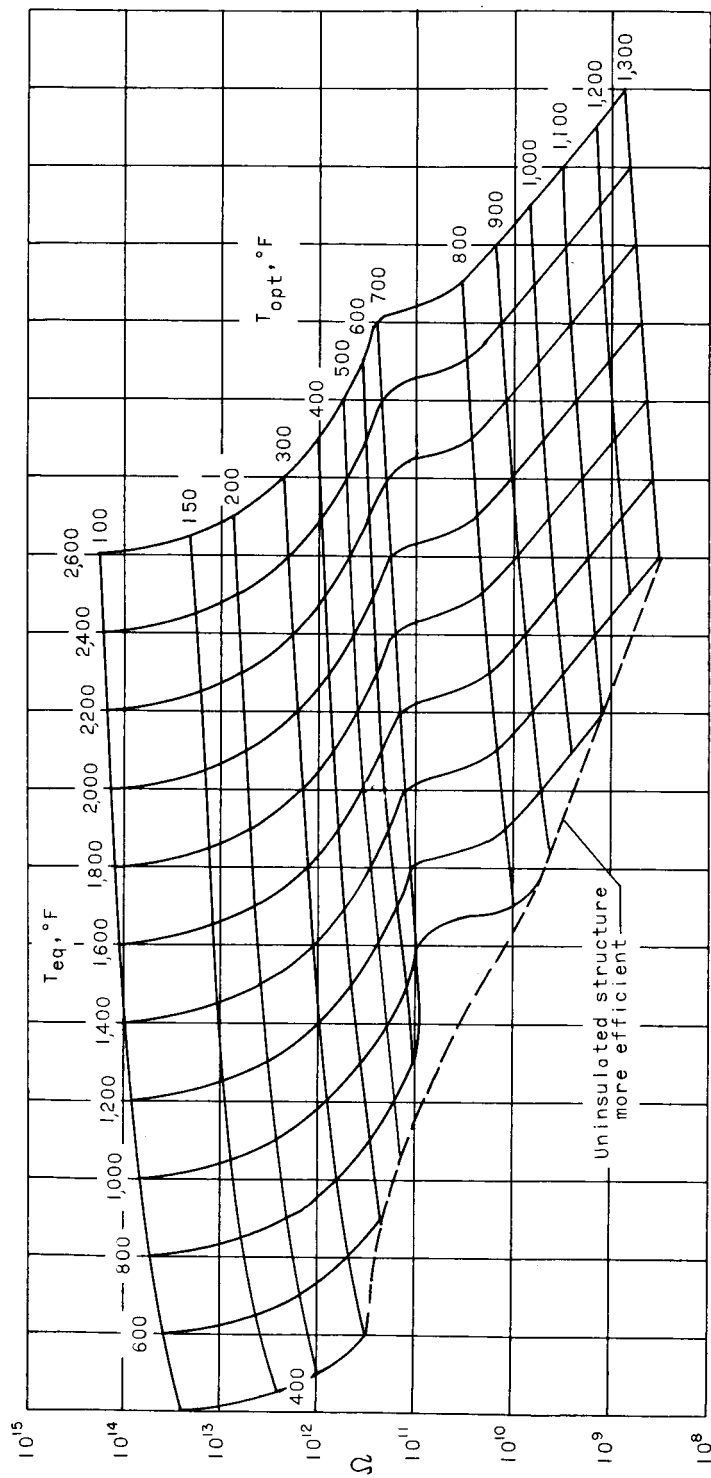


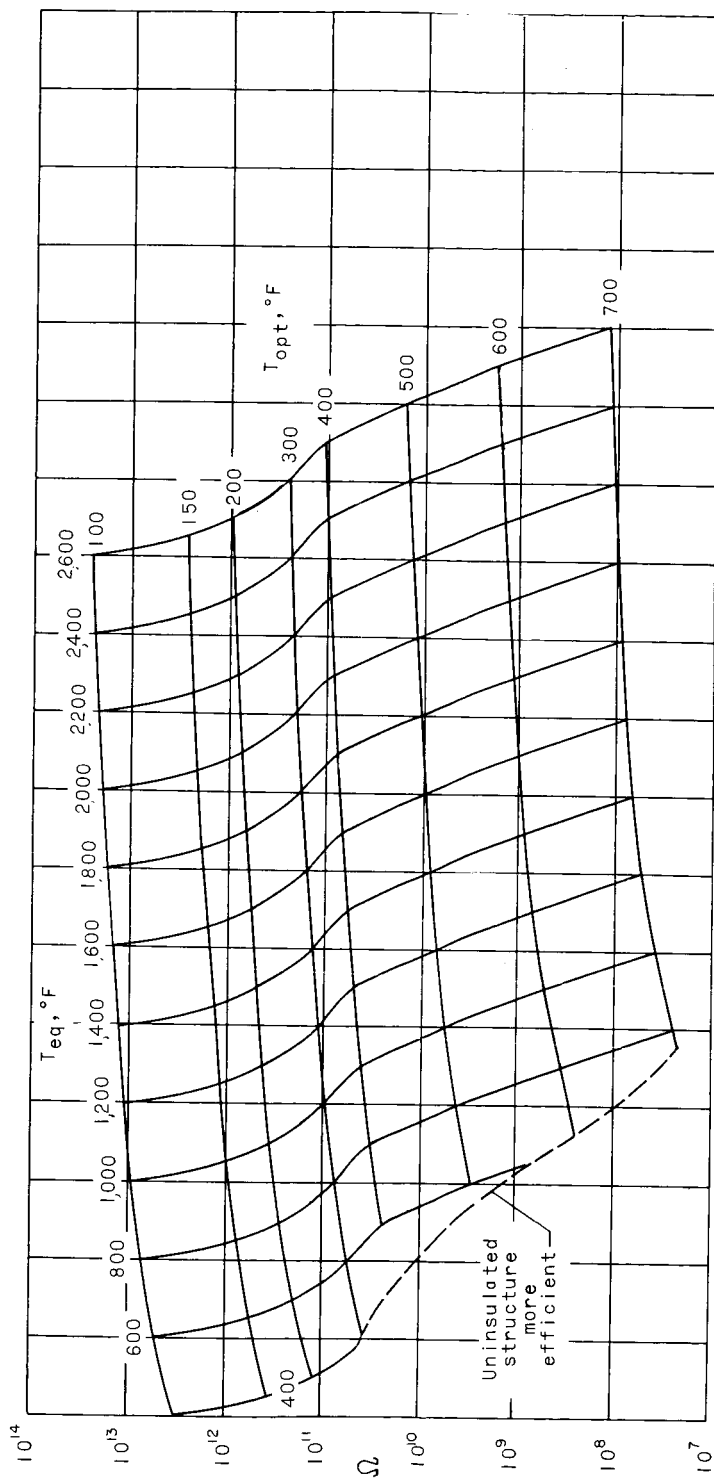
Figure 2.- Yield stress at 0.2-percent offset plotted against temperature. The curves express the analytic approximation to the experimental data.





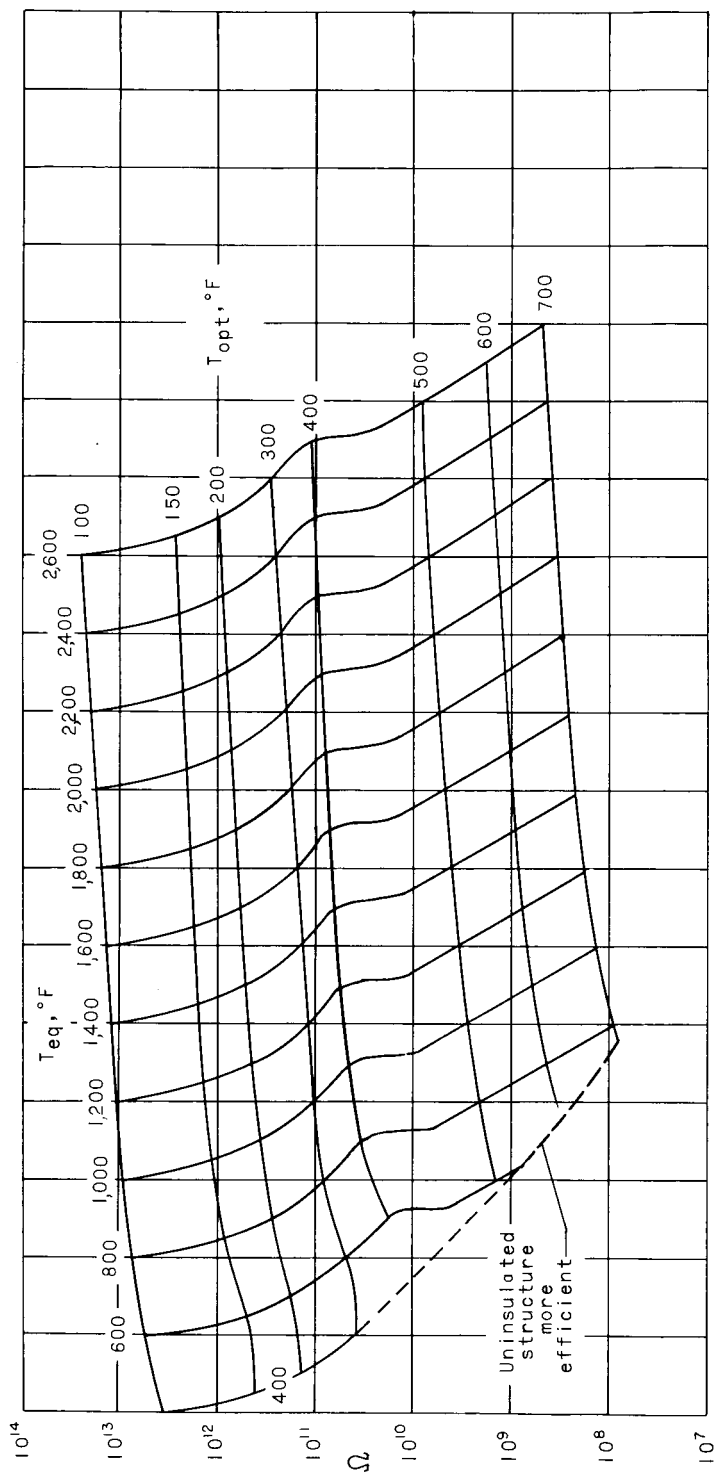
(a) Beryllium.

Figure 3.- The load parameter  $\Omega$  plotted against equilibrium temperature and optimum temperature. The curves are based on an initial temperature of 75° F.



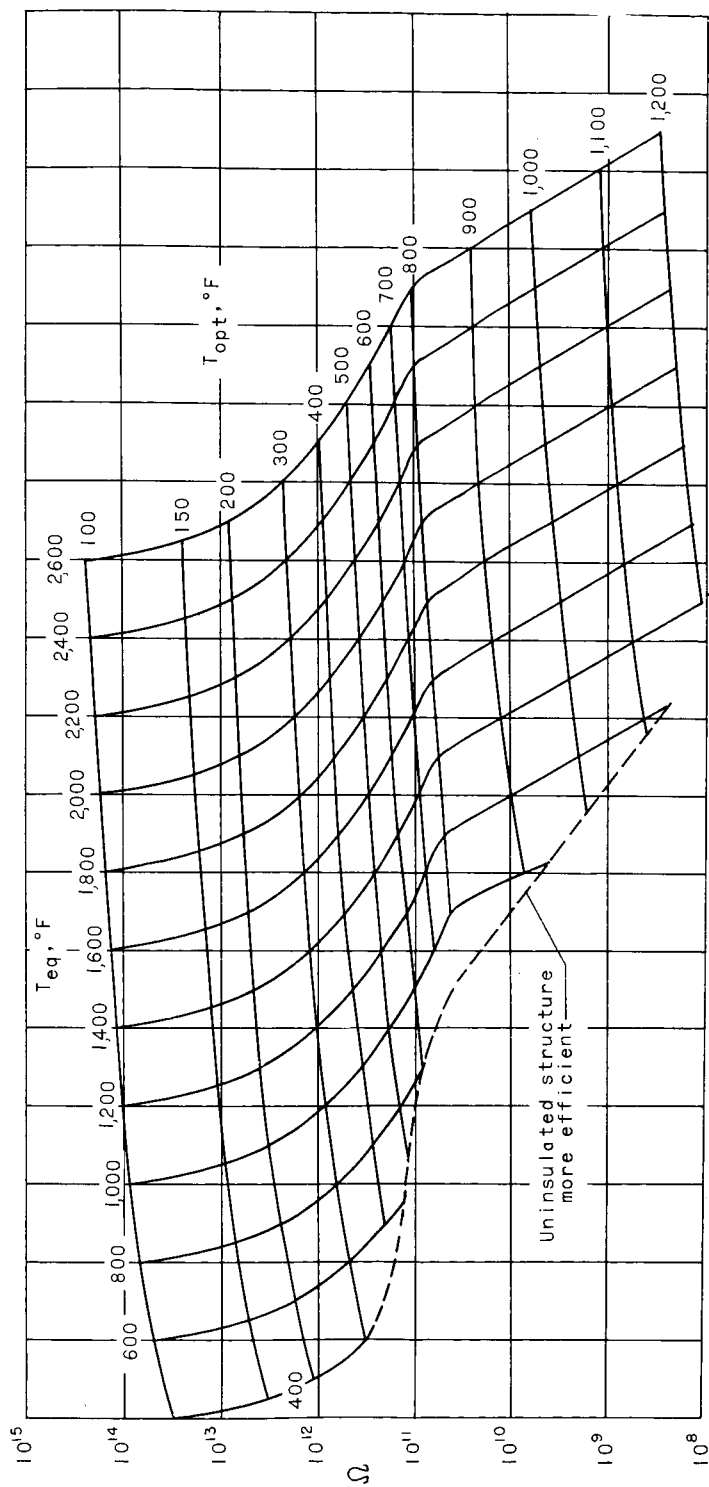
(b) HK31A magnesium alloy.

Figure 3.- Continued.



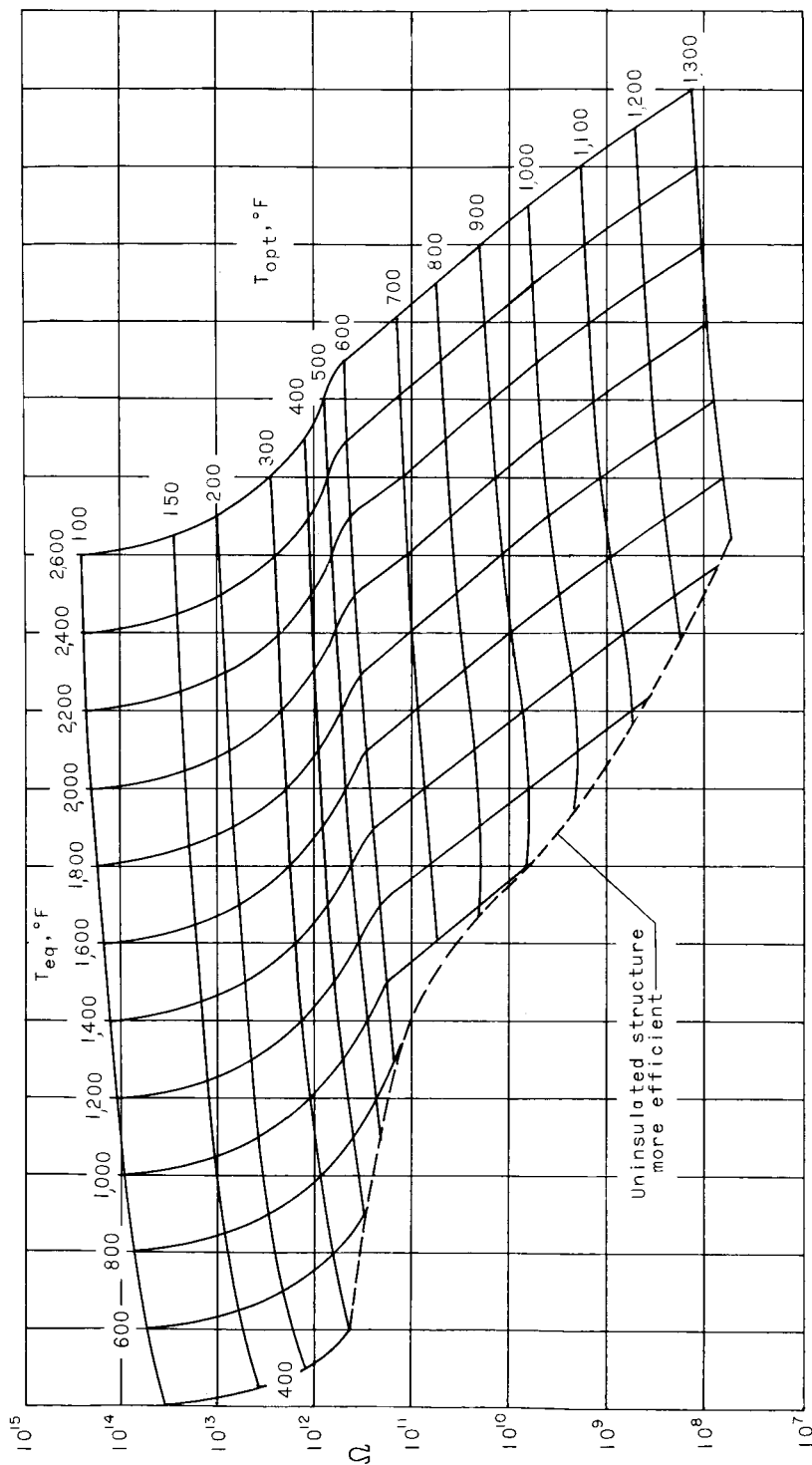
(c) 2024-T4 aluminum alloy.

Figure 3.- Continued.



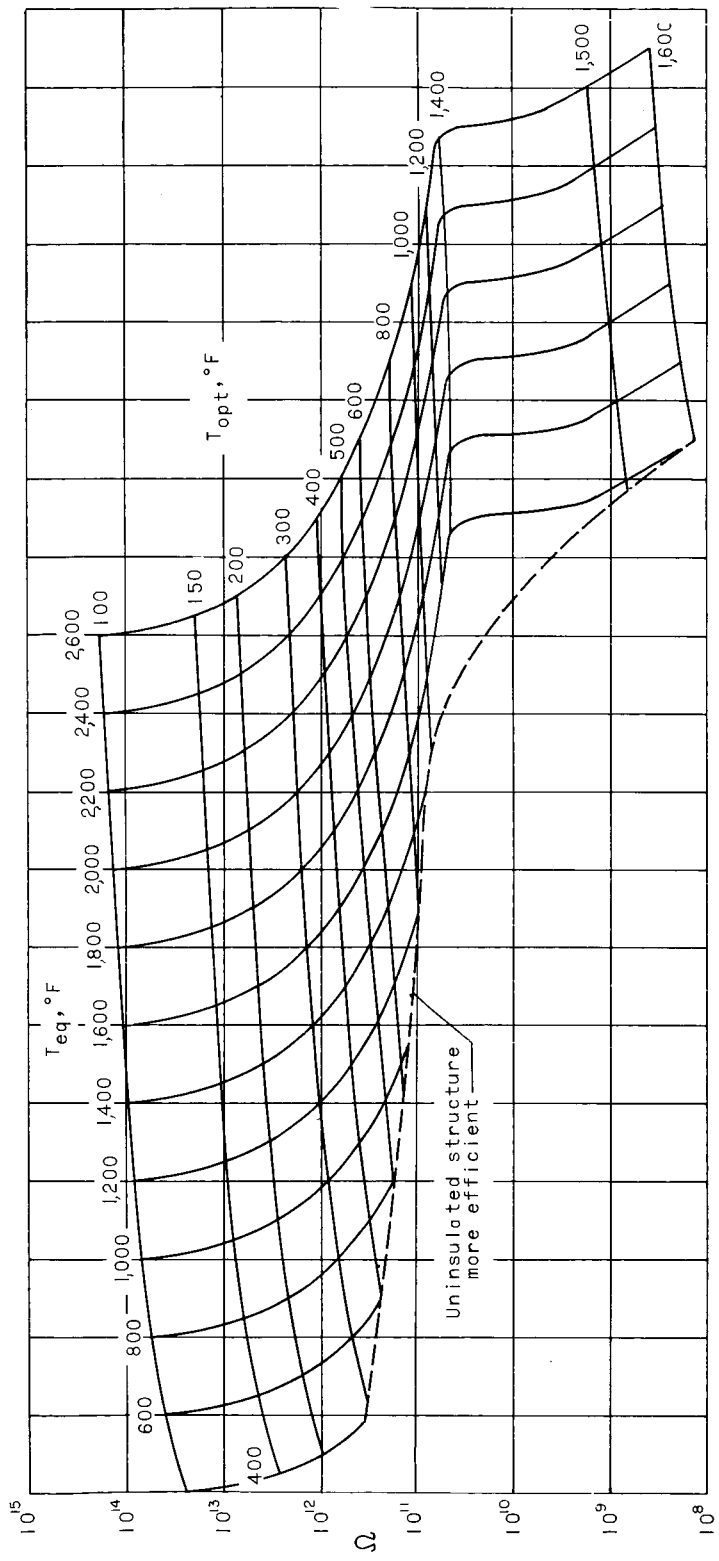
(d) MST 185 titanium alloy.

Figure 3.- Continued.



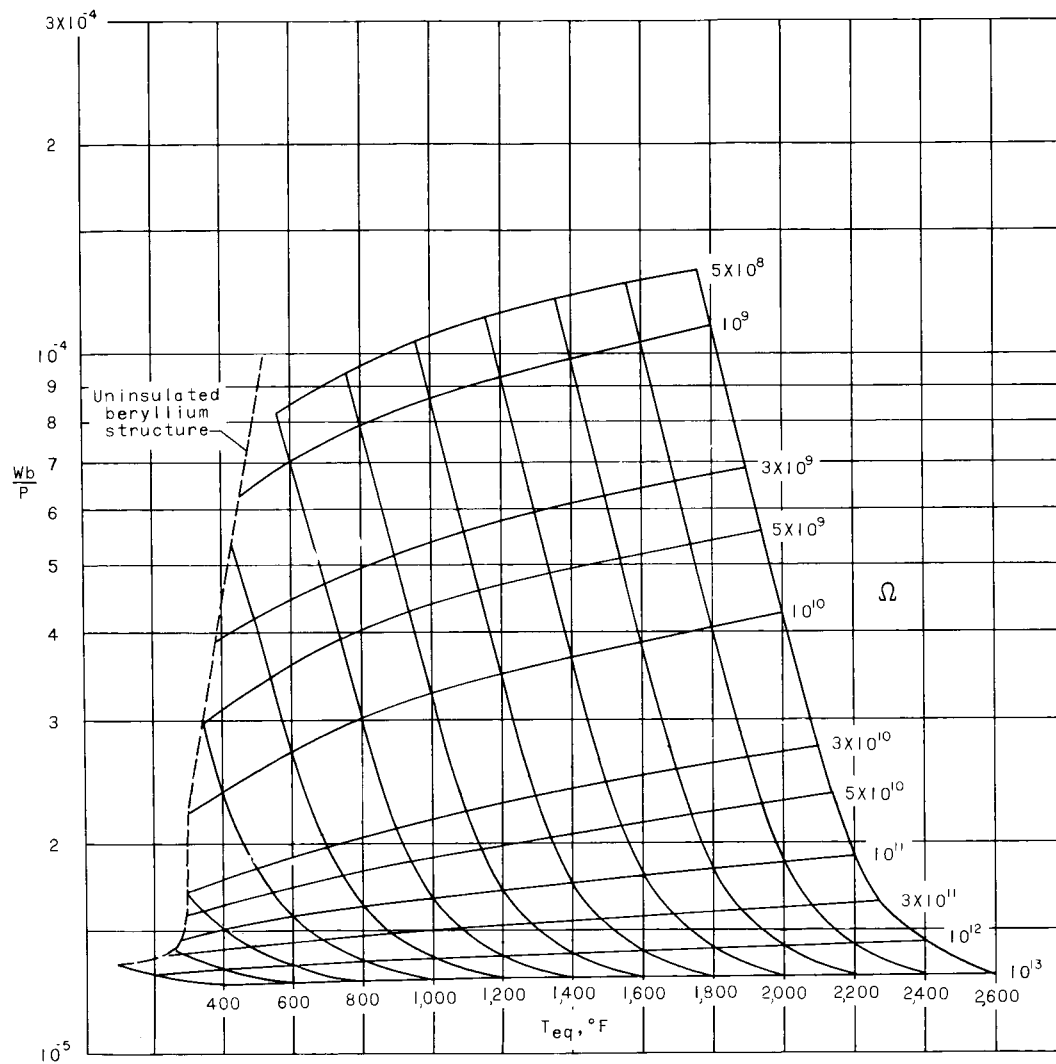
(e) 17-7 PH stainless steel.

Figure 3.- Continued.



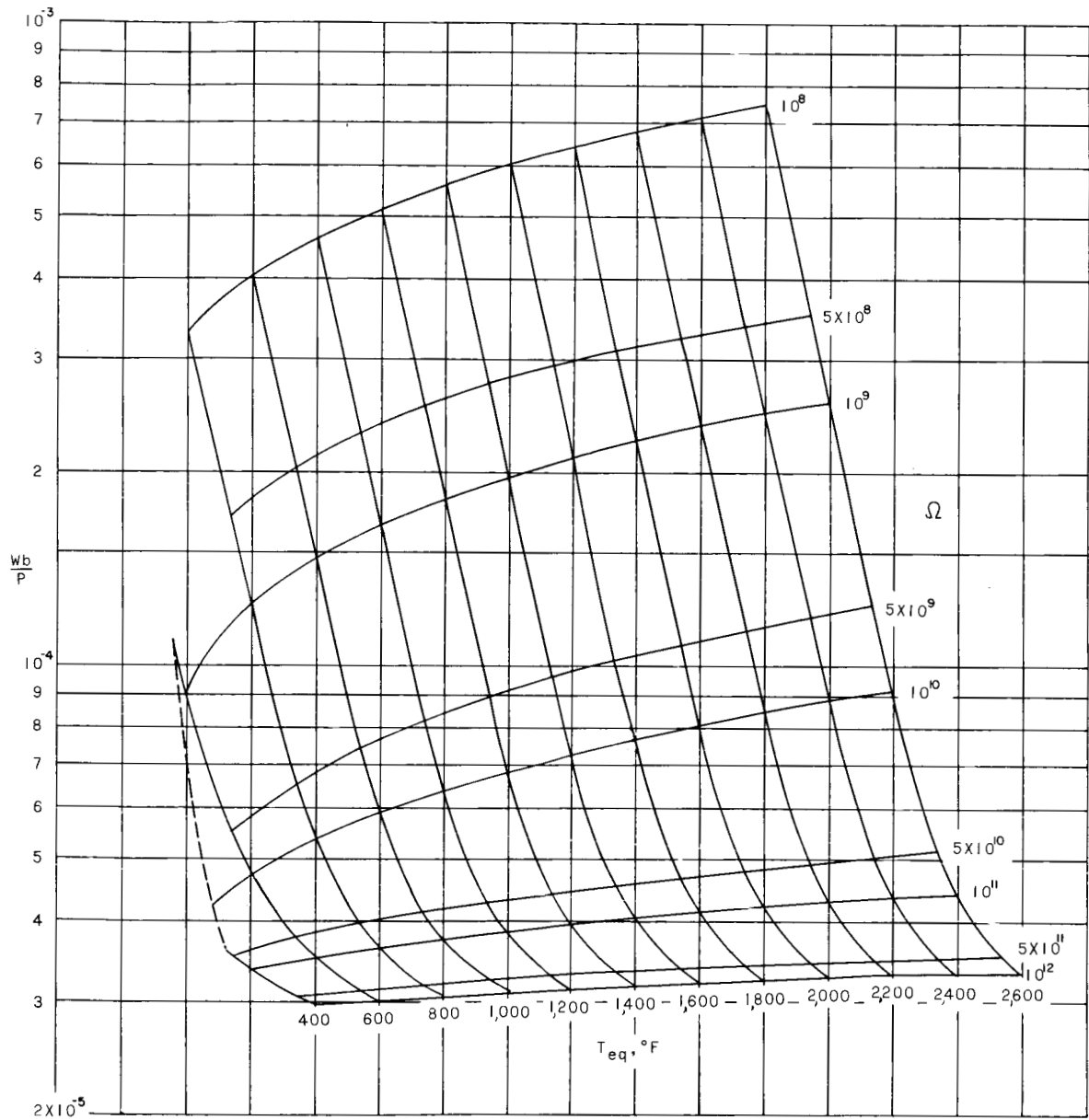
(f) Inconel X.

Figure 3.- Concluded.



(a) Beryllium.

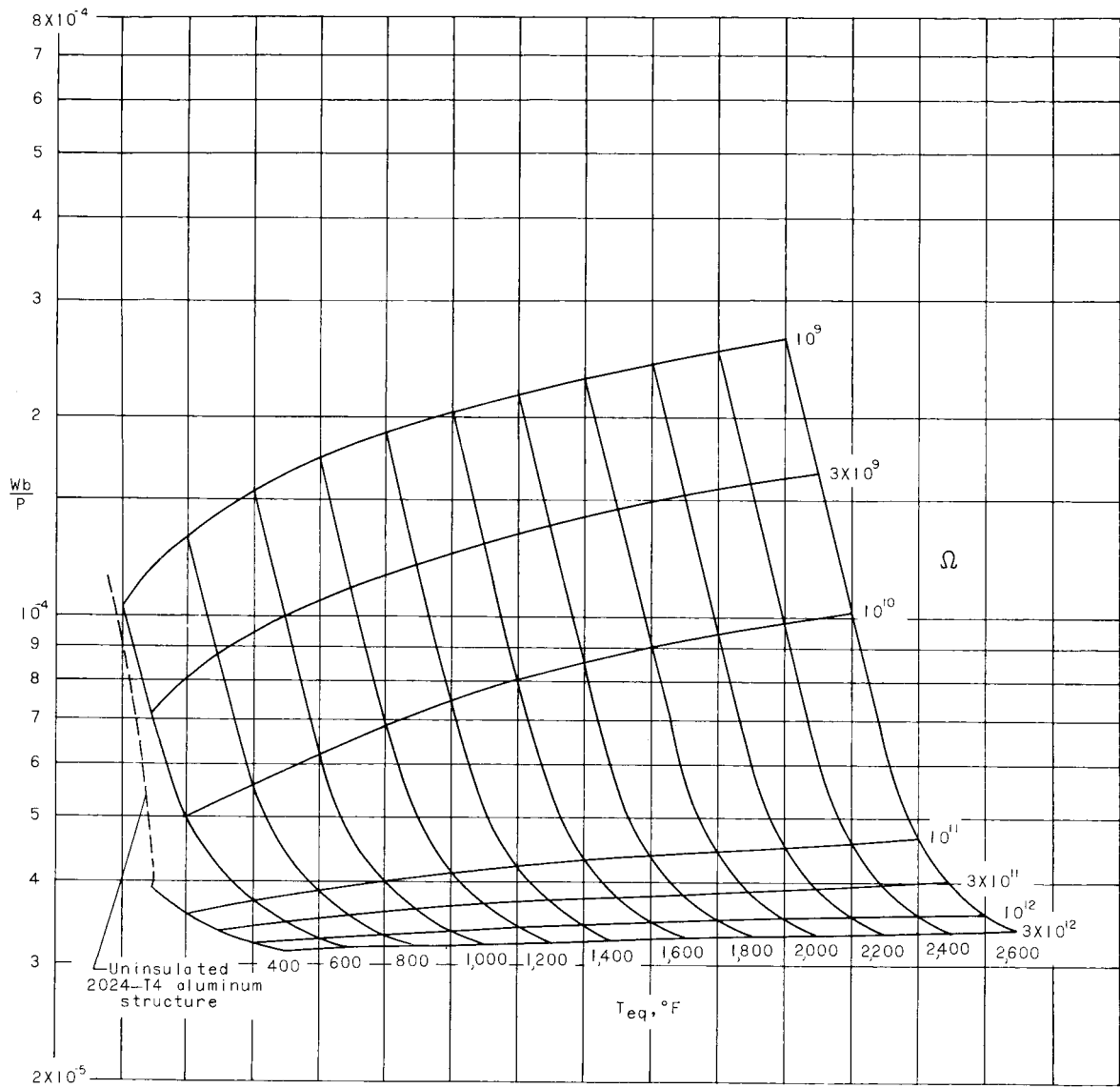
Figure 4.- Weight of optimum tension members plotted against  $T_{eq}$  and  $\Omega$ . The charts are based on an initial temperature of  $75^{\circ}\text{F}$ .



(b) HK31A magnesium alloy.

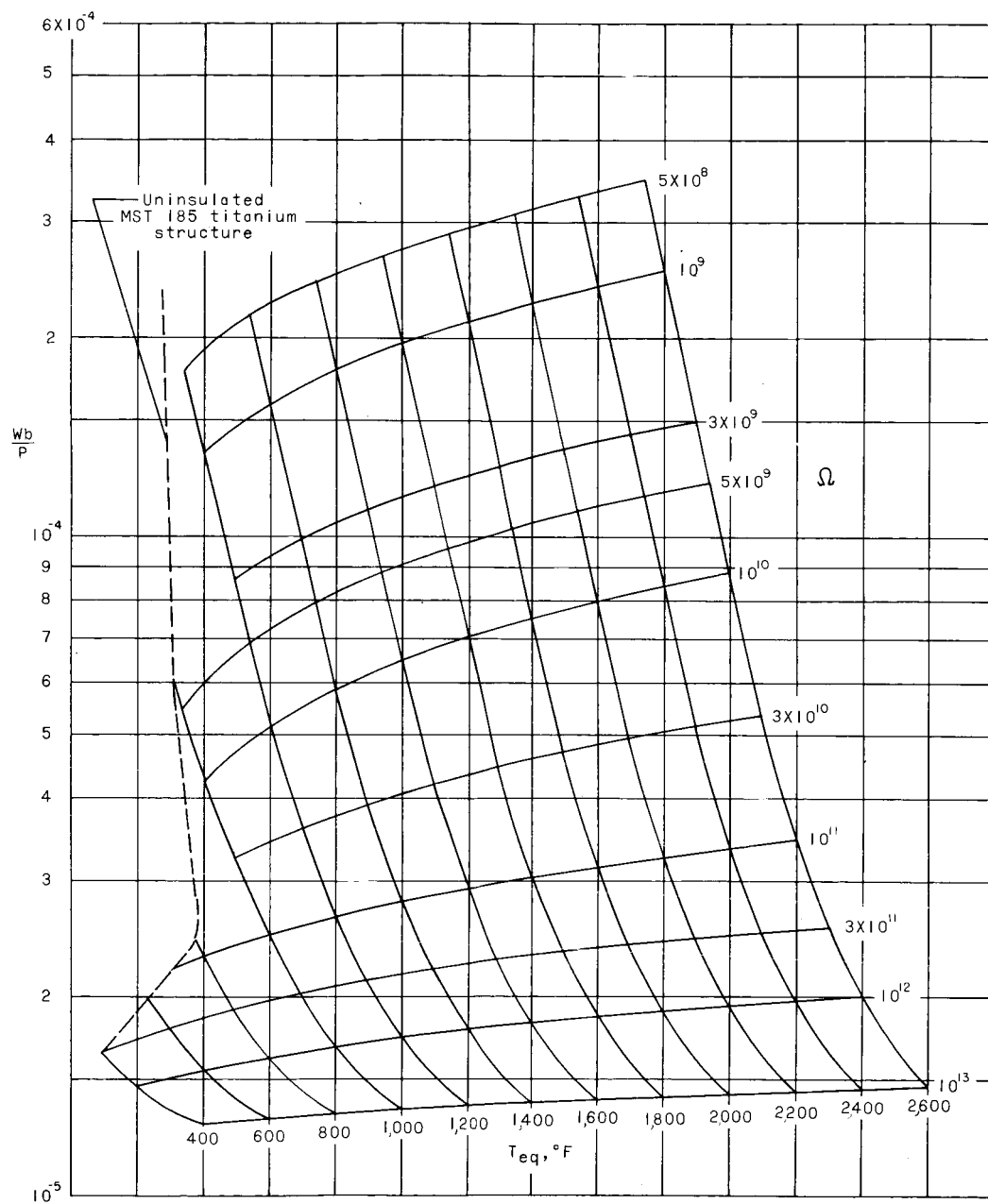
Figure 4.- Continued.





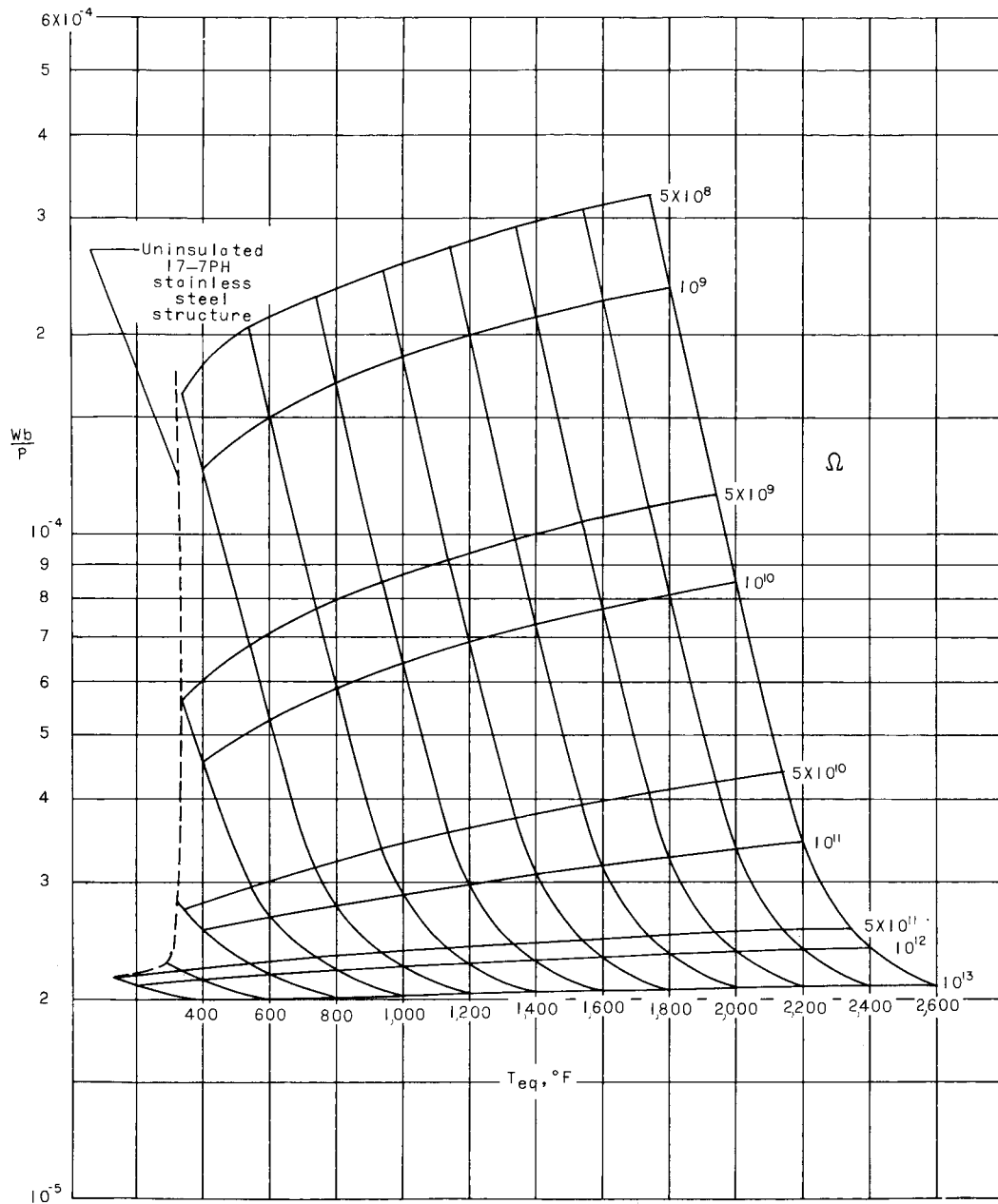
(c) 2024-T4 aluminum alloy.

Figure 4.- Continued.



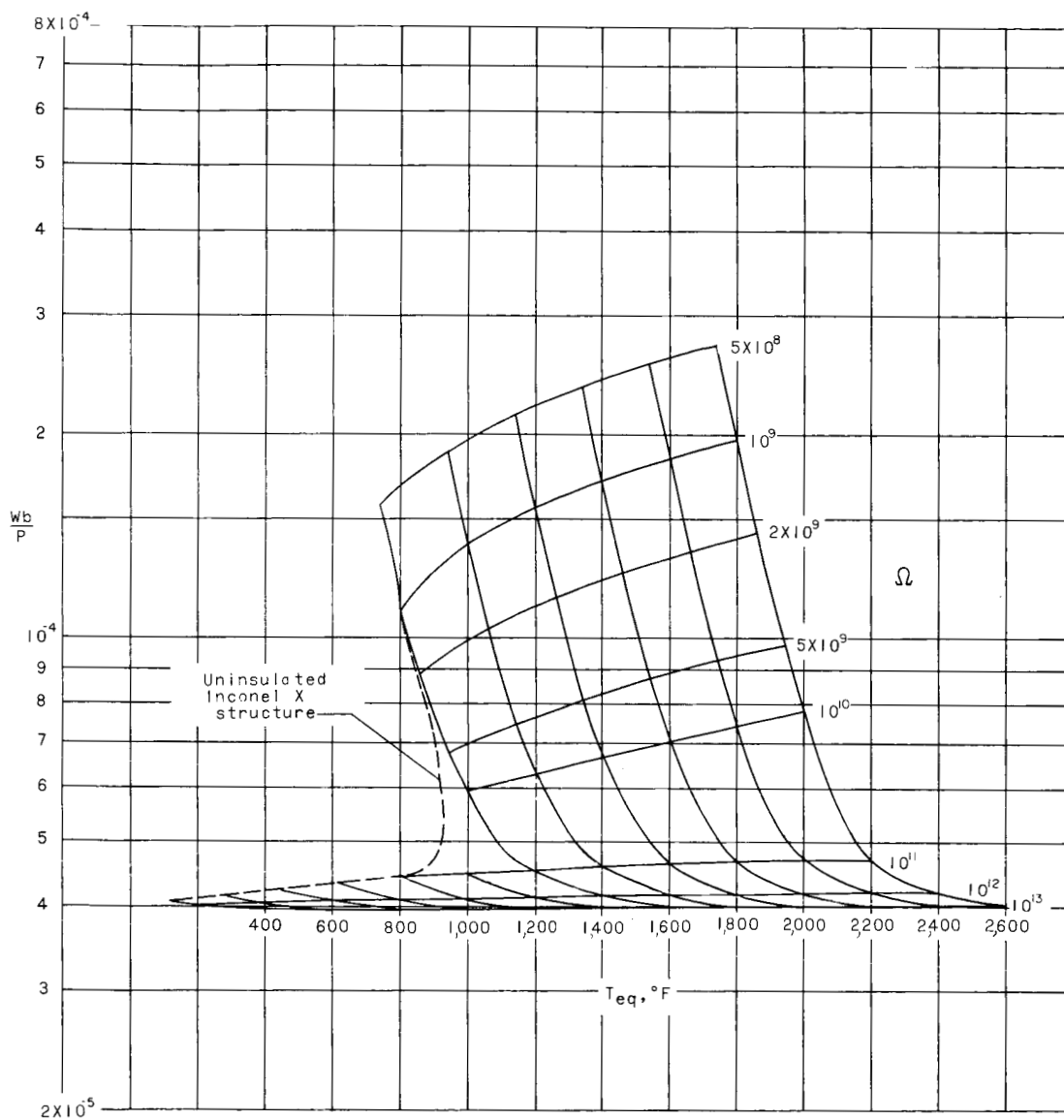
(d) MST 185 titanium alloy.

Figure 4.- Continued.



(e) 17-7 PH stainless steel.

Figure 4.- Continued.



(f) Inconel X.

Figure 4.- Concluded.

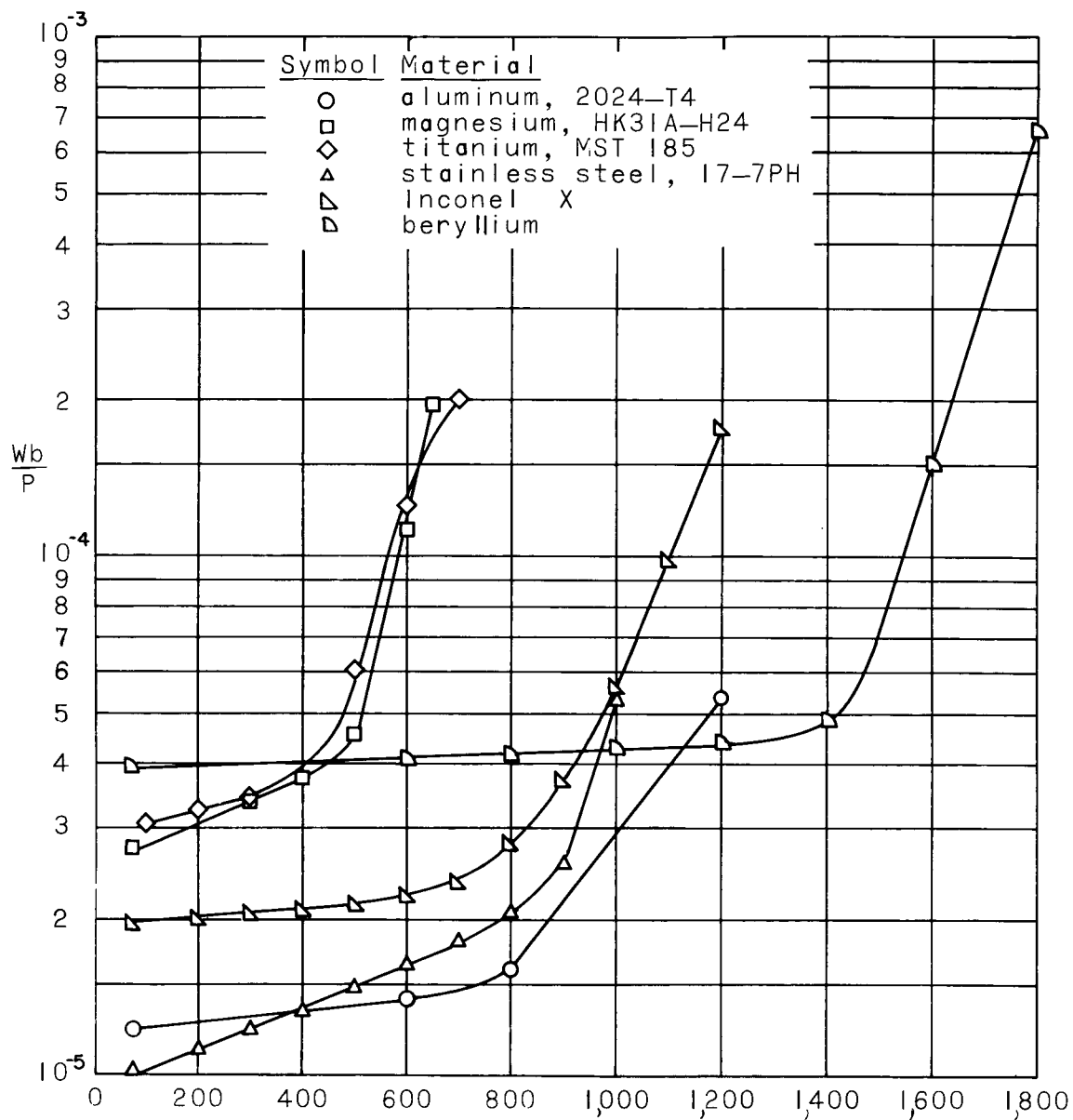


Figure 5.- Efficiency of uninsulated tension members of various materials. It is assumed that the uninsulated structure reaches the equilibrium temperature during the time of flight.

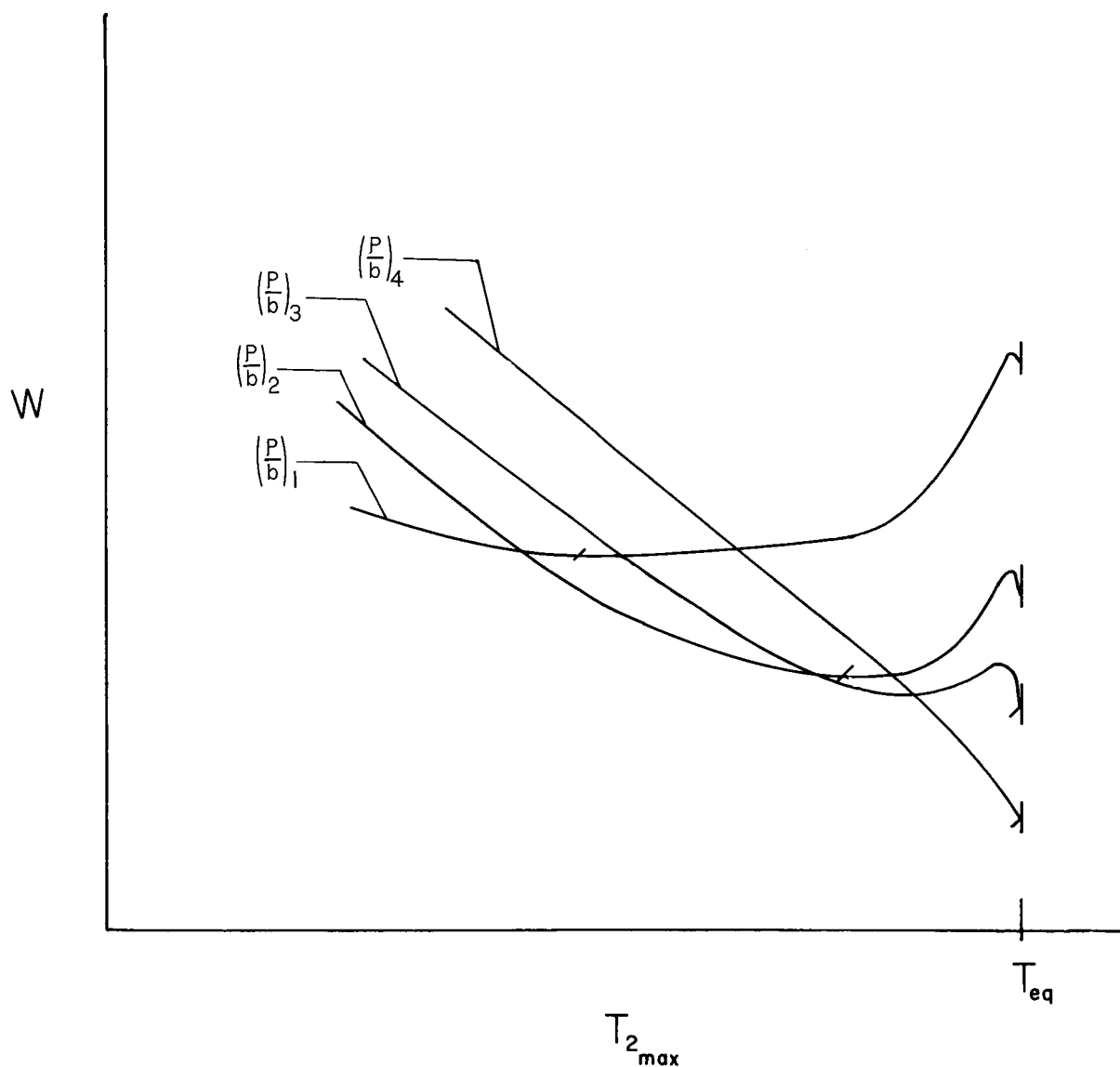


Figure 6.- Total structural weight plotted against structure temperature and load. The tick marks indicate the minimum weight point. The figure is not drawn to scale.  $(P/b)_1 > (P/b)_2 > \dots > (P/b)_4$ .  $(T_2)_{max}$  is the maximum structure temperature which occurs at the end of flight.

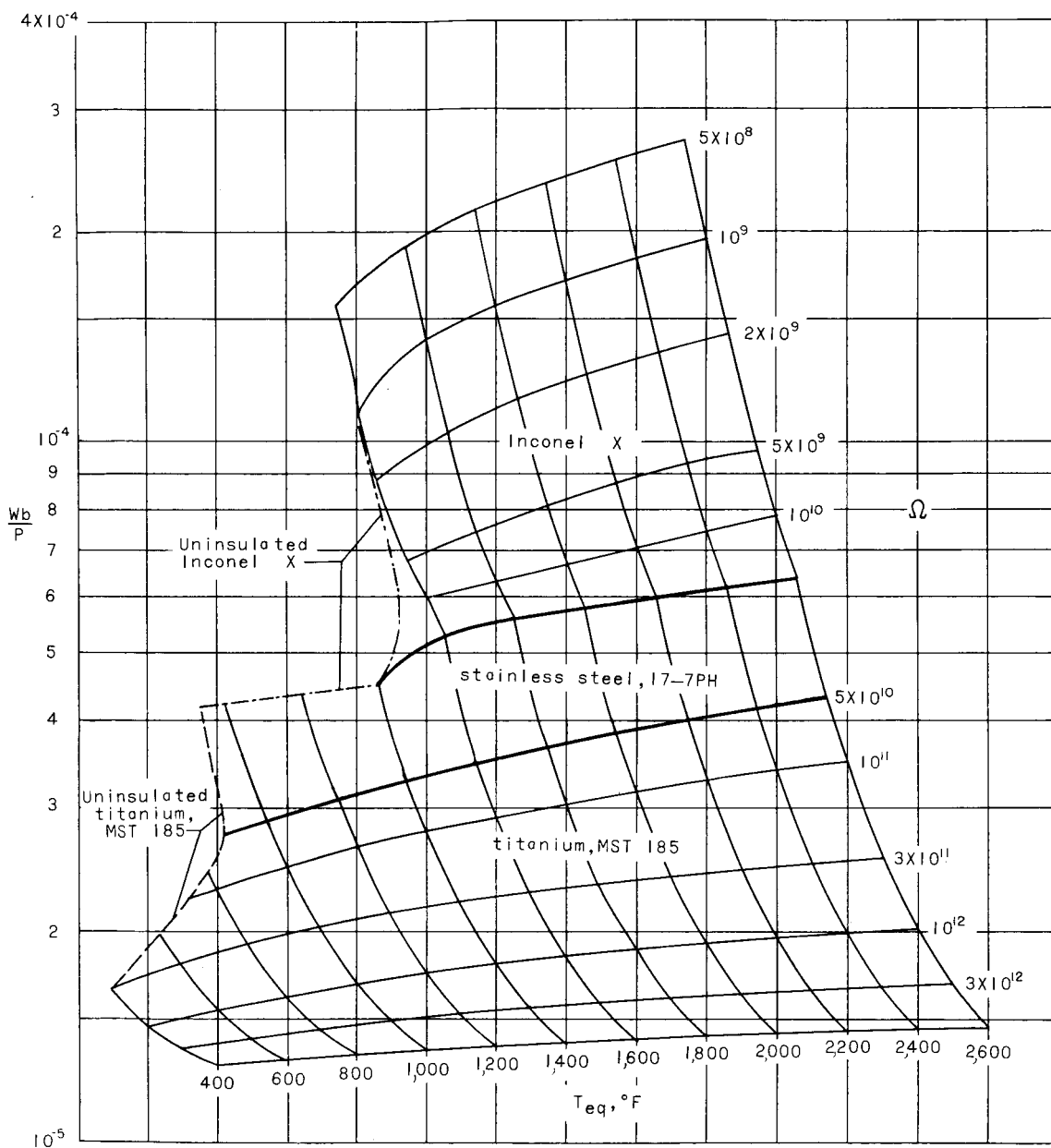


Figure 7.- Composite chart which shows the weight of optimum structures which are the most efficient in specific areas of  $T_{eq}$  and  $\Omega$ . The chart is based on an initial temperature of  $75^\circ F$ .